Int. J. Radiation Oncology Biol. Phys., Vol. 53, No. 2, pp. 353–359, 2002

0360-3016/02/$–see front matter

PII S0360-3016(02)02705-0

CLINICAL INVESTIGATION **Cervix**

MEASUREMENT OF TUMOR VOLUME BY PET TO EVALUATE PROGNOSIS IN PATIENTS WITH ADVANCED CERVICAL CANCER TREATED BY RADIATION THERAPY

TOM R. MILLER, M.D., PH.D.,* AND PERRY W. GRIGSBY, M.D.†

*Mallinckrodt Institute of Radiology and †Department of Radiation Oncology,
Washington University School of Medicine, St. Louis, MO

Purpose: This study evaluated the usefulness of tumor volume measurement with positron emission tomography (PET) in patients with advanced cervical cancer treated by radiation therapy.
Methods and Materials: Fifty-one patients underwent PET before treatment. Primary tumor volume was determined, and volume, FIGO stage, and presence of lymph nodes on the PET study were compared to progression-free survival (PFS) and overall survival (OS).
Results: Tumor volume, lymph node disease, and stage were predictive of PFS, whereas volume and lymph node involvement predicted OS. Lymph node status did not correlate with volume. Dividing patients according to whether the tumor volume was more or less than 60 cm^3 predicted PFS and OS. Separation of patients with tumor volumes ≤60 cm^3 and no lymph node disease vs. any other combination was strongly predictive of PFS and OS.
Conclusions: The following conclusions were drawn regarding patients with advanced cervical cancer treated with radiation therapy: (*1*) Tumor volume can be accurately measured by PET; (*2*) Tumor volume separates patients with a good prognosis from those with a poorer prognosis; (*3*) A subset of patients with relatively small tumors and no lymph node involvement does remarkably well; (*4*) Tumor volume does not correlate with the presence of lymph node disease. © 2002 Elsevier Science Inc.

Cervical cancer, Positron emission tomography, ^{18}F FDG.

INTRODUCTION

Positron emission tomography (PET) employing the radiopharmaceutical ^{18}F fluorodeoxyglucose (FDG) is used in staging and follow-up of a wide variety of cancers, including lymphoma, malignant melanoma, and carcinomas of the esophagus, breast, lung, and colon (e.g., Refs. 1–3). Work from our institution (4, 5) and elsewhere (6–8) has shown that PET is also valuable in staging patients with cervical carcinoma. FDG-PET readily identifies the primary tumor and accurately assesses spread to lymph nodes and distant metastases.

It is well established that tumor size is an important prognostic factor in patients with cervical carcinoma (9, 10). Although clinical stage also is an important factor, stage does not necessarily correlate with tumor size. The limited reliability of physical examination for estimation of size has led to interest in tumor measurement based on three-dimensional imaging techniques (11–15). The work presented here is an attempt to increase the already substantial value of PET in patients with advanced cervical cancer by addition of information about the size of the primary tumor. A quantitative technique is described that accurately measures the tumor volume, with the results showing a strong correlation with treatment outcome, especially when combined with detection of lymph node disease.

METHODS AND MATERIALS

Patients and treatment

Fifty-one consecutive patients with newly diagnosed advanced cervical carcinoma whose digital data were available were included in this retrospective study. All patients were to be treated by radiation therapy. The patients underwent PET imaging for clinical indications before treatment between January 1998 and September 1999. They were treated exclusively with irradiation and, in 29 patients, concurrent cisplatin-based chemotherapy (16). The radia-

Reprint requests to: Tom R. Miller, M.D., Ph.D., Mallinckrodt Institute of Radiology, 510 S. Kingshighway Boulevard, St. Louis, MO 63110 USA. Tel: (314) 362-2809; Fax: (314) 362-2806; E-mail: millert@mir.wustl.edu

This project was supported in part by Grant No. R01 CA85797 from the National Institutes of Health. This work is solely the responsibility of the authors and does not necessarily represent the official views of the National Institutes of Health.

Acknowledgments—We are grateful to Katherine Trinkaus, Ph.D., for help with the statistical analysis and to Patsa Hungspreugs and Jason Jacob for their work with data analysis.

Received Sep 27, 2001, and in revised form Dec 20, 2001. Accepted for publication Dec 27, 2001.

tion therapy consisted of 6 weeks of external beam irradiation with two intracavitary (brachytherapy) treatments during external beam treatment. The total dose to point A, including both external beam and brachytherapy, was 85 Gy, whereas the maximum desired doses to the bladder, rectum, and lateral surface of the vagina were 75, 70, and 130 Gy, respectively.

PET imaging

All patients underwent the standard PET imaging protocols at our institution, consisting of fasting for at least 4 hours, followed by placement of a Foley catheter, i.v. hydration, and administration of 20 mg of furosemide to minimize bladder activity. Then 10–15 mCi (370–555 MBq) ^{18}F FDG was injected with imaging beginning 40–90 min later with a 47-slice ECAT-EXACT PET tomograph (Siemens/CTI, Knoxville, TN). Four to six bed positions were employed to encompass the chest, abdomen, and pelvis. At each position, emission images were obtained for 10 min, along with 2-min transmission images. A segmentation algorithm was used to generate the transmission map (17). Transaxial slices were reconstructed by the ordered-subsets expectation-maximization iterative algorithm (18), followed by Butterworth filtering. The data were collected in a 128 $\times$ 128-pixel matrix with pixel size of 4.3 $\times$ 4.3 mm and a slice spacing of 4.3 mm. The typical reconstructed spatial resolution was 10 mm full-width half-maximum.

Volume measurement

We developed a technique to quantify the three-dimensional volume of the primary tumor by PET (19, 20). This approach involves detection of the boundary of the tumor by simple count thresholding. More sophisticated methods were not needed because of the high target:background ratio of the tumor, typically 10:1 or greater. Tumor tissue was identified on the FDG-PET images as any voxel in the three-dimensional data set with counts greater than a fixed threshold fraction of the peak activity in the tumor. The threshold level was selected by correlation with CT scans performed in 13 patients within 2 weeks of the PET study in which the tumor was clearly delineated from the adjacent normal tissues. The maximum anteroposterior and lateral dimensions of the tumor were determined by visual inspection of the CT scans; from the PET data, the dimensions were determined automatically. To prevent the inclusion of adjacent intense structures, such as the bladder, lymph nodes, and bowel, the tumor region was expanded from a single seed-voxel within the tumor by the region-growing morphologic operation (21). After region growing, any remaining extraneous activity above the threshold was manually eliminated with use of a rapid interactive program. Adjacent activity, particularly in the bladder, required this manual operation in only about one-fourth of cases. This low occurrence was the result, at least in part, of using a Foley catheter and diuresis. The tumor volume was then determined by counting the number of voxels within the thresholded margin of the tumor and multiplying by the known volume of a single voxel.

Lymph node evaluation

PET studies were interpreted in a standard clinical manner, often including correlation with CT. The presence of lymph nodes was evaluated on the pretreatment PET scans. Each study was graded as follows: 0 (no nodes), 1 (pelvic nodes only), 2 (pelvic and para-aortic nodes), and 3 (pelvic, para-aortic, and supraclavicular nodes). The PET lymph node findings in a larger group, which included all of these patients, have been reported previously (5).

Follow-up

Clinical follow-up examinations were performed 6 weeks after completion of treatment and subsequently at 3-month intervals. For this analysis, two distinct end points were used: progression-free survival (PFS) and overall survival (OS). PFS was computed as the time interval from initiation of radiation therapy to the time of first recurrence or the last follow-up visit, whereas OS was the time from beginning of treatment to death or the last follow-up.

Statistical analysis

Survival analysis was performed by the Kaplan–Meier approach (22). The multivariate Cox proportional hazards model was used to assess the separate and joint effects of tumor volume, lymph node status, and FIGO stage on recurrence and OS. Statistical significance was assessed by the log–rank or Wald tests. The correlation of tumor volume and lymph node grade was assessed by analysis of variance (ANOVA) (22). The volume was also computed in patients with and without lymph node disease and compared with a *t* test. Correlation of tumor volume and FIGO stage was computed similarly. Linear regression was employed for the correlation of tumor dimensions by PET and CT.

RESULTS

A typical example of the PET/CT correlation used to validate the PET edge detector is presented in Fig. 1. The slice best demonstrating the maximum dimensions of the primary tumor is shown, along with marks indicating the boundaries of the tumor. To retain maximum spatial resolution, the CT dimensions were measured directly from film and not from the interpolated, digitized images shown in the figure.

The results for a threshold value of 40% are shown in Fig. 2, along with the correlation coefficient ($r = 0.88$) and best-fit line for the 13 patients (26 data points). The correlation coefficients and fits were similar for a threshold value of 30%, but the volumes were higher than those seen in published surgical series; there was also a much more bothersome inclusion of bladder activity, requiring manual removal. Therefore, the 40% value was preferred. Note that there is no significant inter- or intraobserver error, because

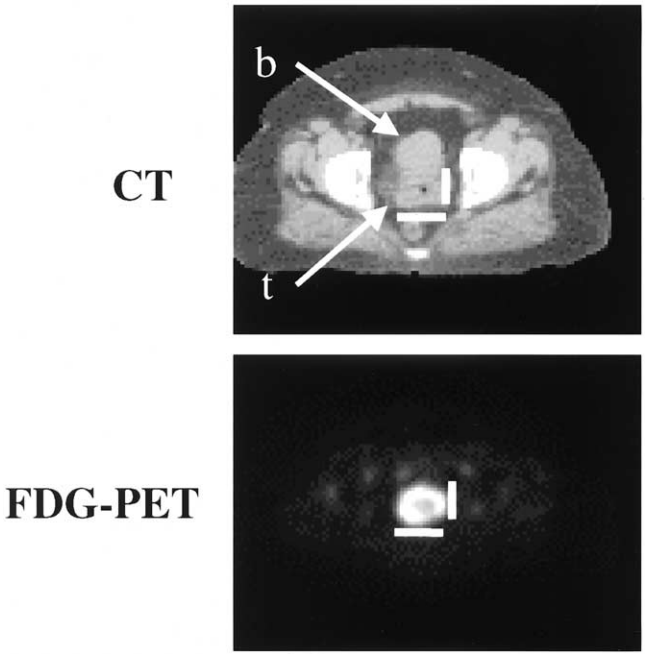

Fig. 1. Selected transaxial slices from a representative CT and PET study are shown. The primary tumor (t) and bladder (b) are identified on the CT, and the anteroposterior and lateral dimensions are indicated by bars.

the calculation is completely automatic, except for the infrequent need to manually exclude bladder activity.

The clinical characteristics, imaging results, and survival for the 51 patients are given in Table 1. The patients ranged in age from 24 to 87 years (mean: 49 years). They were followed 0.2–3.1 years (mean: 1.7 years). Eighteen patients experienced a recurrence, with 17 dying of their disease during the follow-up period. Primary tumor volumes ranged from 0 to 216 cm^3 (mean: 60 cm^3). Thirty-two patients had

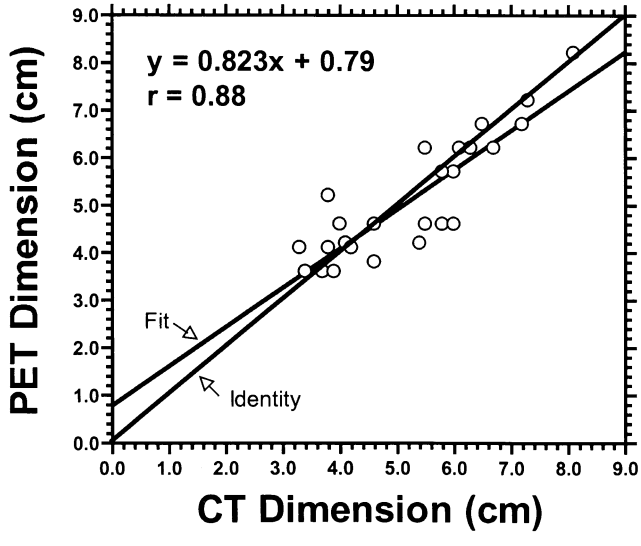

Fig. 2. The anteroposterior and lateral dimensions from the CT scans and the FDG-PET studies are shown for the 26 data points, along with the best-fit line and the line of identity.

lymph node involvement by PET, whereas 19 did not. Twelve patients were FIGO Stage I, 25 were Stage II, 13 were Stage III, and 1 was Stage IV. Two patients had adenocarcinoma, 3 adenosquamous carcinoma, and 46 squamous cell carcinoma.

Tables 2 and 3 summarize the survival analysis and the correlations with tumor volume. Tumor volume was predictive of both progression-free survival ($p = 0.005$) and overall survival ($p = 0.003$) by Cox analysis. To further elucidate the effects of tumor volume, a cutoff point was determined by generation of histograms of the tumor volumes for patients with and without recurrence or death. A volume of 60 cm^3 well separated the two groups. The Kaplan–Meier graph is shown in Fig. 3 for progression-free survival, with patients divided into those with relatively small tumor volumes ($V \leq 60$ cm^3 [$n = 34$]) and larger volumes ($V > 60$ cm^3 [$n = 17$]). The difference was statistically significant ($p = 0.007$). Figure 4 shows OS for patients in both volume groups. Again, the difference was significant ($p = 0.003$).

Correlation of the grading of lymph node site with volume was not significant ($p = 0.50$) by ANOVA. The primary tumor volumes for patients with and without lymph node disease were 63 ± 48 cm^3 and 56 ± 52 cm^3, respectively, an insignificant difference ($p = 0.64$) by the t test. Previously published work (5) analyzing much of the same image data demonstrated a correlation between disease in lymph nodes and PFS that was marginally confirmed in this smaller subset of patients ($p = 0.06$). In this study, the correlation with overall survival was significant ($p = 0.04$).

Tumor volume correlation with FIGO stage was statistically significant by both ANOVA ($p = 0.03$) and the t test ($p = 0.001$). For the 37 patients with Stage I or II disease, the volume was 47 ± 37 cm^3, whereas for the 14 Stage III or IV patients, the volume was 96 ± 60 cm^3. Separating patients by disease stage (Stage I or II vs. Stage III or IV) was, however, not predictive of progression-free survival ($p = 0.09$) or overall survival ($p = 0.10$).

The results for the Cox multivariate survival analysis are shown in Table 4. Volume is treated as a continuous variable, lymph node disease is considered to be present or absent, and FIGO stage is dichotomized as Stage I or II vs. Stage III or IV. Both tumor volume and lymph node disease were predictive of progression-free survival and overall survival, whereas stage did not add additional prognostic information when the other factors were taken into account.

Noting that both volume and lymph node involvement were predictive of recurrence and death, but not correlated with each other, an additional Kaplan–Meier analysis of the combination of these factors was performed. Figure 5 shows the analysis of progression-free survival for a subset of patients ($n = 14$) that had small tumor volumes (≤ 60 cm^3) and no lymph node disease (Group I) and for a second group with larger volumes, lymph node involvement, or both ($n = 37$ [Group II]) ($p = 0.01$). Of the 14 patients (7%) in Group I, one experienced recurrence over a follow-up period 571–968 days, whereas 17 (46%) of Group II patients had

Table 1. Patient characteristics

Number	Stage	Histology	Age (yr)	LN	Volume (cm^3)	Status	PFS (days)	OS (days)
1	IIb	Squamous	43	−	9	AWD	622	832
2	IIIb	Squamous	45	+	216	DOD	96	322
3	IIb	Squamous	61	+	40	DOD	151	342
4	IIb	Adenosq	44	+	47	DOD	95	466
5	IIb	Squamous	27	+	89	DOD	211	275
6	Ib2	Adenosqu	56	+	47	DOD	337	397
7	IIIb	Squamous	52	+	84	DOD	103	384
8	Ib2	Squamous	24	+	24	DOD	188	270
9	IVb	Squamous	38	+	172	DOD	132	149
10	IIIb	Squamous	40	+	25	DOD	80	138
11	IIb	Squamous	67	−	96	DOD	196	252
12	IIIb	Squamous	47	+	133	DOD	55	55
13	IIb	Squamous	43	+	43	DOD	160	177
14	IIb	Squamous	52	−	84	DOD	213	239
15	Ib2	Squamous	38	+	81	DOD	104	195
16	Ib2	Squamous	45	+	46	DOD	265	730
17	IIIb	Squamous	34	+	113	DOD	99	334
18	IIIb	Squamous	48	−	160	DOD	345	429
19	IIb	Squamous	47	+	10	NED	1017	1017
20	Ib2	Squamous	28	+	65	NED	498	498
21	IIb	Squamous	28	−	48	NED	615	615
22	IIIb	Squamous	31	+	109	NED	616	616
23	IIIb	Squamous	47	+	104	NED	1131	1131
24	IIb	Squamous	54	−	21	NED	894	894
25	IIIb	Adenosqu	49	+	46	NED	704	704
26	IIb	Squamous	58	+	39	NED	732	732
27	IIIb	Squamous	27	−	44	NED	752	752
28	Ib1	Squamous	47	+	0	NED	961	961
29	IIb	Squamous	55	−	15	NED	703	703
30	Ia1	Adeno	53	−	0	NED	968	968
31	IIb	Squamous	71	+	34	NED	988	988
32	IIb	Squamous	47	+	107	NED	643	643
33	Ib2	Squamous	39	+	34	NED	1096	1096
34	IIb	Adeno	45	+	50	NED	883	1040
35	IIb	Squamous	83	−	9	NED	661	661
36	IIb	Squamous	42	−	57	NED	571	571
37	Ib2	Squamous	47	−	42	NED	703	703
38	IIb	Squamous	48	+	32	NED	1015	1015
39	IIIb	Squamous	71	−	36	NED	596	596
40	Ib2	Squamous	29	+	15	NED	799	799
41	IIb	Squamous	43	+	24	NED	826	826
42	IIIb	Squamous	44	−	14	NED	761	761
43	IIb	Squamous	56	−	54	NED	830	830
44	IIb	Squamous	57	−	53	NED	730	730
45	IIIb	Squamous	65	+	84	NED	1050	1050
46	IIb	Squamous	54	−	108	NED	614	614
47	Ib2	Squamous	60	−	27	NED	902	902
48	IIb	Squamous	87	+	29	NED	154	154
49	IIb	Squamous	63	+	40	NED	622	622
50	Ib1	Squamous	71	−	192	NED	788	788
51	Ib2	Squamous	36	+	33	NED	382	382

Abbreviations: LN = lymph node disease (positive or negative); PFS = progression-free survival; OS = overall survival; AWD = alive with disease; DOD = dead of disease; NED = no evidence of disease; Adenosq = adenosquamous; Adeno = adenocarcinoma.

recurrence in fewer than 346 days ($p = 0.01$). Figure 6 shows the overall survival for the two groups. No deaths were recorded for the Group I patients over the 968-day maximum follow-up period, whereas 17 (46%) of the Group II patients died, 16 within 466 days and 1 at 730 days. A *p*-value could not be computed for this last evaluation of overall survival, because there were no deaths in Group I (All of those patients yielded "censored" data points). Comparison with the progression-free survival analysis in Fig. 5 indicates that for overall survival, the statistical significance of the finding should be at least as great.

A similar analysis, but with the two groups divided into those with nodal disease and large tumors ($n = 12$) vs. all others ($n = 39$), also yielded statistically significant results

Table 2. Survival analysis

	p-value	
	PFS	OS
Tumor volume	0.005	0.003
Volume ≤60 cm^3 vs >60 cm^3	0.007	0.003
Lymph nodes positive vs. negative	0.06	0.04
Stage I or II vs. Stage III or IV	0.09	0.10
Group I vs. Group II*	0.01	†

Abbreviations: PFS = progression-free survival; OS = overall survival.

* Group I: V ≤60 cm^3 and negative lymph nodes; Group II: all others.

† See text.

($p = 0.01$ for progression-free survival, and $p = 0.02$ for overall survival), but with survival curves not markedly different from those for volume alone.

DISCUSSION

Failure of initial treatment with radiation therapy is associated with a poor salvage rate and reduced long-term survival in patients with advanced cervical carcinoma. It is critically important that the initial course of therapy be effective, because many studies show that the primary cause of poor long-term survival after definitive radiotherapy is failure to achieve local control (e.g., Refs. 23–25). Thus, ways are needed to identify patients at high risk who may be candidates for more aggressive initial treatment.

MRI has been extensively evaluated in recent years in patients with cervical carcinoma. MRI is superior to physical examination and ultrasonography in staging (26), and contrast enhancement techniques provide additional prognostic information (13, 27) and may permit assessment of tumor oxygenation (28). Several studies have shown that measurement of tumor volume by MRI is accurate and valuable in estimation of prognosis (11–15).

The success of PET in employing the radiolabeled glucose analog ^{18}F fluorodeoxyglucose (FDG-PET) in staging and follow-up of many tumors led our group (4, 5) and others (6–8) to evaluate its use in cervical cancer. FDG-PET is now established as a useful imaging study in the initial staging and follow-up of these patients. In a recent study, Grigsby *et al.* (5) demonstrated that FDG-PET detects abnormal lymph nodes with greater frequency than CT and that lymph node involvement is strongly predictive of survival.

Table 3. Correlation with tumor volume

	Volume (cm^3)	*p*-value
Lymph nodes positive	63 ± 48	0.64*
Lymph nodes negative	56 ± 52	
Stage I or II	47 ± 37	0.001†
Stage III or IV	96 ± 60	

* Lymph nodes positive vs. negative.

† Stage I or II vs. Stage III or IV.

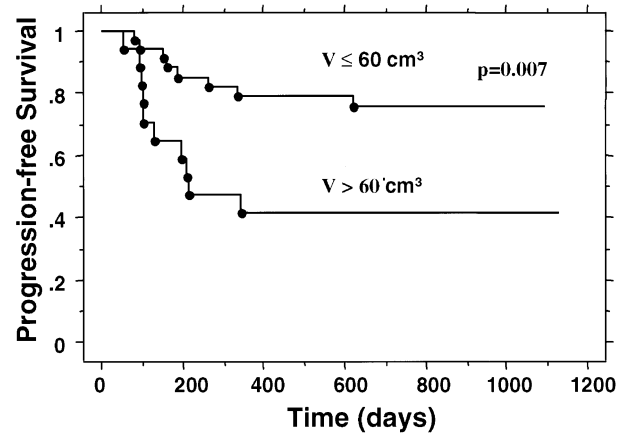

Fig. 3. Progression-free survival is shown for patients with relatively small volumes, $V \leq 60$ cm^3 ($n = 34$) and larger volumes, $V > 60$ cm^3 ($n = 17$).

The well-established role of tumor size in predicting survival in patients with cervical carcinoma (e.g., Refs. 9, 10, 12–15), combined with the recently demonstrated value of PET, led to the development of a quantitative technique to measure the volume of the primary tumor as an adjunct to the PET evaluation of lymph nodes. This computerized approach provides an objective, reproducible measure, validated against CT, requiring only modest user interaction.

This volume measurement differs from most previous work in that the image data are treated three-dimensionally, rather than as one or more two-dimensional transaxial slices. This approach also employs an automatic edge detection algorithm without manual intervention, except for elimination of adjacent bowel and bladder activity in approximately one-fourth of cases. This edge

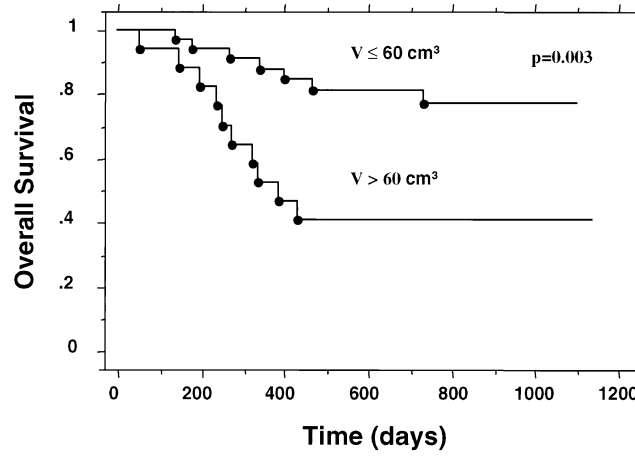

Fig. 4. Overall survival is shown for patients with relatively small volumes, $V \leq 60$ cm^3 ($n = 34$) and larger volumes, $V > 60$ cm^3 ($n = 17$).

Table 4. Combined effect of multiple variables on survival

Parameter	*p*-value PFS	*p*-value OS
Volume*	0.01	0.01
Lymph nodes positive vs. negative	0.05	0.05
Stage I or II vs. III or IV	0.76	0.99

Abbreviations: PFS = Progression-free survival; OS = Overall survival.

* Continuous variable.

detection was achieved by a simple thresholding approach made possible by the very high tumor:background ratio, typically greater than 10:1. Region growing from a "seed" voxel within the tumor minimized detection of activity outside the primary tumor volume.

A principal finding of this work is that tumor volume is strongly correlated with progression-free survival and overall survival (Table 2 and Figs. 3 and 4) in patients with advanced cervical cancer treated by radiation therapy. The previously reported observation in many of these same patients, that lymph node status also predicted survival (5), was noted.

Interestingly, although both volume and lymph node status are strongly predictive of survival, they are not correlated with each other (Table 3) in these patients with advanced cervical cancer. Thus, it is reasonable to suspect that they are independent predictors of survival that may be even more effective when combined. This, indeed, was found to be the case. As shown in Figs. 5 and 6, only one of the patients with a small tumor who was without lymph node disease experienced recurrence, and no patients died during the follow-up period. In contrast, patients with other combinations of those factors suffered recurrence or death at rates not significantly different from those determined by volume alone.

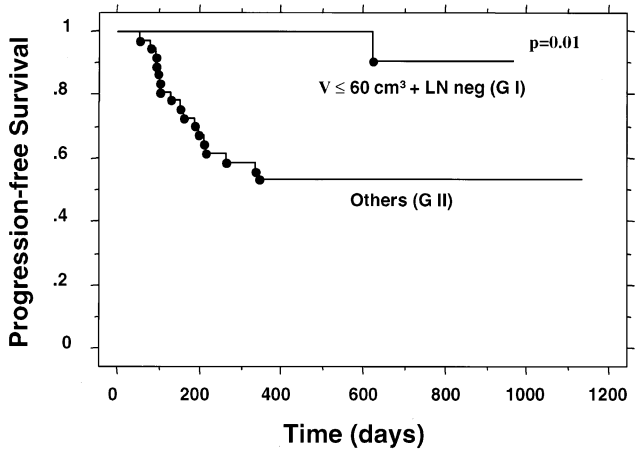

Fig. 5. Progression-free survival is shown for a subset of patients (n = 14) that had small tumor volumes (≤60 cm^3) and no lymph node disease (Group I) and for a second group with larger volumes, lymph node involvement, or both (n = 37 [Group II]).

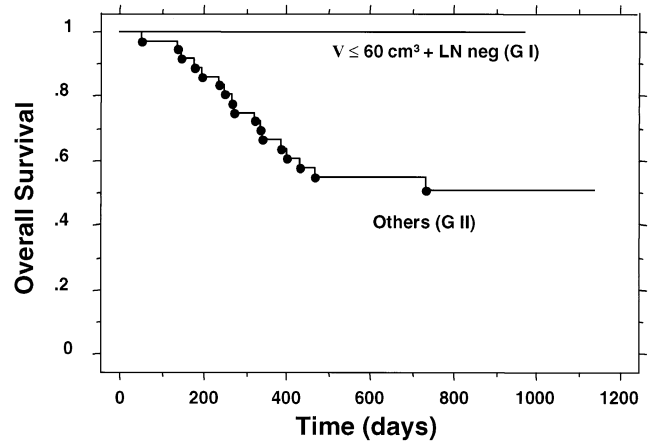

Fig. 6. Overall survival is shown for the Group I and Group II patients, defined in the text and in the caption to Fig. 5.

This observed powerful effect of tumor volume and lymph node disease in the absence of a correlation between them may have a reasonable explanation that reflects the inherent biologic characteristics of the tumors. As shown here and elsewhere, patients with large tumors fare more poorly than those with small tumors, and patients with lymph node spread also have a worse prognosis. Perhaps the group with the most favorable prognosis has tumors with cells that divide slowly and are of a type that does not readily spread beyond the primary tumor. Patients who do less well may have more aggressive tumors that spread to lymph nodes early, before the tumor becomes large. Another group of tumors may be less aggressive, growing over a long period of time to become large, eventually also leading to a poor prognosis at the time of eventual presentation for treatment.

Thus, patients with small tumors who are free of lymph node involvement at the time of diagnosis—a significant fraction of our study population—do remarkably well after treatment. It may be that those patients can be reassured at the time of initial treatment that they have an excellent prognosis. Perhaps more importantly, the other patients who do much more poorly may be candidates for more aggressive initial treatment.

In conclusion, in this study of patients with advanced cervical cancer treated by radiation therapy: (*1*) Tumor volume can be accurately measured by PET; (*2*) Quantitative measurement of tumor volume separates patients with a good prognosis from those with a poorer prognosis; (*3*) A subset of patients with relatively small tumors and no lymph node involvement does remarkably well; (*4*) Tumor volume does not correlate with the presence of disease in lymph nodes. Thus, FDG-PET with measurement of tumor volume and assessment of lymph node status identifies patients with a poor prognosis who may require more aggressive initial treatment to prevent recurrence and death.

REFERENCES

1. Conti PS, Lilien DL, Hawley K, *et al*. PET and 18F-FDG in oncology: A clinical update. *Nucl Med Biol* 1996;23:717–735.
2. Rigo P, Paulus P, Kaschten B, *et al*. Oncological applications of positron emission tomography with fluorine-18 fluorodeoxyglucose. *Eur J Nucl Med* 1996;23:1641–1674.
3. Gambhir SS, Czernin J, Schwimmer J, *et al*. A tabulated summary of the FDG PET literature. *J Nucl Med* 2001;42:1S-93S.
4. Grigsby PW, Dehdashti F, Siegel BA. FDG-PET evaluation of carcinoma of the cervix. *Clin Positron Imag* 1999;2:105–109.
5. Grigsby PW, Siegel BA, Dehdashti F. Lymph node staging by positron emission tomography in patients with carcinoma of the cervix. *J Clin Oncol* 2001;19:3745–3749.
6. Rose P, Adler L, Rodriguez M, *et al*. Positron emission tomography for evaluating para-aortic nodal metastasis in locally advanced cervical cancer before surgical staging: A surgicopathologic study. *J Clin Oncol* 1999;17:41–45.
7. Sugawara Y, Eisbruch A, Kosuda S, *et al*. Evaluation of FDG-PET in patients with cervical cancer. *J Nucl Med* 1999; 40:1125–1131.
8. Reinhardt M, Ehritt-Braun C, Vogelgesang D, *et al*. Metastatic lymph nodes in patients with cervical cancer: Detection with MR imaging and FDG PET. *Radiology* 2001;218:776–782.
9. Stehman FB, Bundy BN, SiSaia PJ, *et al*. Carcinoma of the cervix treated with radiation therapy. I. A multi-variate analysis of prognostic variables in the Gynecologic Oncology Group. *Cancer* 1991;67:2776–2785.
10. Perez C, Grigsby P, Chao K, *et al*. Tumor size, irradiation dose, and long-term outcome of carcinoma of uterine cervix. *Int J Radiat Oncol Biol Phys* 1998;41:307–317.
11. Mayr N, Magnotta V, Ehrhardt J, *et al*. Usefulness of tumor volumetry by magnetic resonance imaging in assessing response to radiation therapy in carcinoma of the uterine cervix. *Int J Radiat Oncol Biol Phys* 1996;35:915–924.
12. Mayr N, Yuh W, Zheng J, *et al*. Tumor size evaluated by pelvic examination compared with 3-D MR quantitative analysis in the prediction of outcome for cervical cancer. *Int J Radiat Oncol Biol Phys* 1997;39:395–404.
13. Mayr N, Yuh W, Zheng J, *et al*. Prediction of tumor control in patients with cervical cancer: Analysis of combined volume and dynamic enhancement pattern by MR imaging. *AJR* 1998; 170:177–182.
14. Toita T, Kakinohana Y, Shinzato S, *et al*. Tumor diameter/volume and pelvic node status assessed by magnetic resonance imaging (MRI) for uterine cervical cancer treated with irradiation. *Int J Radiat Oncol Biol Phys* 1999;43:777–782.
15. Hawnaur J, Johnson R, Buckley C, *et al*. Staging, volume estimation, and assessment of nodal status in carcinoma of the cervix: Comparison of magnetic resonance imaging with surgical findings. *Clin Radiol* 1994;49:443–452.
16. Morris M, Eifel PJ, Lu J, *et al*. Pelvic radiation with concurrent chemotherapy compared with pelvic and para-aortic radiation for high-risk cervical cancer. *N Engl J Med* 1999;340: 1137–1143.
17. Xu M, Luk W, Cutler P, *et al*. Local threshold for segmented attenuation correction of PET imaging of the thorax. *IEEE Trans Nucl Sci* 1994;41:1532–1537.
18. Hudson HM, Larkin RS. Accelerated image reconstruction using ordered subsets of projection data. *IEEE Trans Med Imag* 1994;13:601–609.
19. Miller TR, Grigsby PW. Assessment of tumor volume in cervical cancer by F-18 FDG PET (Abstr.). *J Nucl Med* 1999;40:255P.
20. Miller TR, Jacob JS, Hungspreugs P. Quantification of tumor size and uptake by FDG-PET (Abstr.). *J Nucl Med* 2000;40: 60P.
21. Castleman K. Digital image processing. Englewood Cliffs, NJ: Prentice Hall; 1996. p. 468–470.
22. Armitage P, Berry G. Statistical methods in medical research. 2nd ed. Oxford, UK: Blackwell Scientific Publications; 1987. p. 428–433.
23. Suyama S, Nakaguchi T, Kawakami K, *et al*. Computed tomography analysis of causes of local failure in radiotherapy for cervical carcinoma. *Cancer* 1998;83:1956–1965.
24. Perez C, Breaux S, Madfoc-Jones H, *et al*. Radiation therapy alone in the treatment of carcinoma of uterine cervix. I. Analysis of tumor recurrence. *Cancer* 1983;51:1393–1402.
25. Jampolis A, Andras E, Fletcher G. Analysis of sites and causes of failures of irradiation in invasive squamous cell carcinoma of the intact uterine cervix. *Radiology* 1975;115:681–685.
26. Hawnaur J, Johnson R, Carrington B, *et al*. Predictive value of clinical examination, transrectal ultrasound and magnetic resonance imaging prior to radiotherapy in carcinoma of the cervix. *Br J Radiol* 1998;71:819–827.
27. Hricak H, Swift P, Campos Z, *et al*. Irradiation of the cervix uteri: Value of unenhanced and contrast-enhanced MR imaging. *Radiology* 1993;189:381–388.
28. Cooper R, Carrington B, Loncaster J, *et al*. Tumour oxygenation levels correlate with dynamic contrast-enhanced magnetic resonance imaging parameters in carcinoma of the cervix. *Radiother Oncol* 2000;57:53–59.